



Original article

Metabolomics-based comparative analysis of the effects of host and environment on *Viscum coloratum* metabolites and antioxidative activities

Rui-Zhen Zhang^a, Jing-Tao Zhao^b, Wei-Qing Wang^a, Rong-Hua Fan^c, Rong Rong^a, Zhi-Guo Yu^a, Yun-Li Zhao^{a,*}

^a Department of Pharmaceutical Analysis, School of Pharmacy, Shenyang Pharmaceutical University, Shenyang, 110016, China

^b School of Pharmacy, University College London, 29-39 Brunswick Square, Bloomsbury, London, WC1N 1AX, UK

^c Department of Sanitary Inspection, School of Public Health, Shenyang Medical College, Shenyang, 110034, China

ARTICLE INFO

Article history:

Received 19 November 2020

Received in revised form

10 April 2021

Accepted 11 April 2021

Available online 17 April 2021

Keywords:

Viscum coloratum

Host

Environment

Plant metabolomics

Multivariate statistical analysis

Biological activity

ABSTRACT

Viscum coloratum (Kom.) Nakai is a well-known medicinal hemiparasite widely distributed in Asia. The synthesis and accumulation of its metabolites are affected by both environmental factors and the host plants, while the latter of which is usually overlooked. The purpose of this study was to comprehensively evaluate the effects of host and habitat on the metabolites in *V. coloratum* through multiple chemical and biological approaches. The metabolite profile of *V. coloratum* harvested from three different host plants in two habitats were determined by multiple chemical methods including high-performance liquid chromatography-ultraviolet (HPLC-UV), gas chromatography-flame ionization detector (GC-FID) and ultra-performance liquid chromatography quadrupole time of flight mass spectrometry (UPLC-QTOF/MS). The differences in antioxidant efficacy of *V. coloratum* were determined based on multiple in vitro models. The multivariate statistical analysis and data fusion strategy were applied to analyze the differences in metabolite profile and antioxidant activity of *V. coloratum*. Results indicated that the metabolite profile obtained by various chemical approaches was simultaneously affected by host and environment factors, and the environment plays a key role. Meanwhile, three main differential metabolites between two environment groups were identified. The results of antioxidant assay indicated that the environment has greater effects on the biological activity of *V. coloratum* than the host. Therefore, we conclude that the integration of various chemical and biological approaches combined with multivariate statistical and data fusion analysis, which can determine the influences of host plant and habitat on the metabolites, is a powerful strategy to control the quality of semi-parasitic herbal medicine.

© 2021 The Authors. Published by Elsevier B.V. on behalf of Xi'an Jiaotong University. This is an open access article under the CC BY-NC-ND license (<http://creativecommons.org/licenses/by-nc-nd/4.0/>).

1. Introduction

Viscum coloratum (Kom.) Nakai (mistletoe) is a well-known medicinal hemiparasite and is widely distributed in Asia. It has been used as a traditional Chinese medicine (TCM) for a long history in China. According to the basic theory of TCM, *V. coloratum* is used to treat ailments such as arthralgia, soreness of the waist and knees, and threatened abortion. In many pharmacological studies, *V. coloratum* has been confirmed to have various pharmacological

activities, such as treating cardiovascular system diseases [1–3], anti-aging, anti-oxidation [4], and anti-tumor activities [5–7], and immune regulation [8].

Hemiparasites are capable of photosynthesis. Therefore, like other plants, the synthesis and accumulation of its metabolites are affected by environmental factors. For example, the podophyllotoxin content in *Podophyllum hexandrum*, which grows in different natural habitats, varies greatly [9]. After supplementing UV-B radiation, the total content of flavonoids, kaempferol and quercetin

Peer review under responsibility of Xi'an Jiaotong University.

* Corresponding author.

E-mail address: ylzhao@syphu.edu.cn (Y.-L. Zhao).

province, China; warm temperate humid monsoon climate). The sample details are shown in Table 1. The collected plants were placed in a ventilated and dark place, and dried at room temperature. The samples with voucher were stored in the State Key Laboratory of Traditional Chinese Medicine (Shenyang Pharmaceutical University, China).

2.2. Chemicals and reagents

The HPLC-grade acetonitrile and HPLC-grade methanol were bought from Fisher Scientific (Fair Lawn, NJ, USA). Tetrahydrofuran normal hexane and methanol were purchased from Tianjin Concord Co., Ltd. (Tianjin, China). Acetic acid and formic acid (HPLC-grade) were purchased from Shenyang Chemical Reagent Factory (Shenyang, China). Tris (hydroxymethyl) methyl aminomethane, pyrogallol, pyrogallol and benzaldehyde (HPLC-grade) were purchased from Bodi Chemical Engineering Co., Ltd. (Tianjin, China). Potassium phosphate monobasic and dipotassium phosphate were purchased from Xilong Chemical Co., Ltd. (Shantou, China). Hydrochloric acid was purchased from Tianjin Kemiou Chemical Reagent Co., Ltd. (Tianjin, China). 1,1-Diphenyl-2-picrylhydrazyl free radical was purchased from TCI Chemical Industry Development Co., Ltd. (Shanghai, China). Ultrapure water was used throughout this study.

2.3. Sample preparation

V. coloratum was ground into powder that can pass through the #4 mesh sieve. An accurately weighed 1.0 g *V. coloratum* powder was extracted with 25 mL of 50% methanol in a conical flask with plug under sonication for 30 min. Solvent loss was compensated with 50% methanol when the conical flask was cooled. The extracts were centrifuged at 3,000 r/min for 3 min. The supernatant was then filtered using a 0.22 μm filter for HPLC analysis. The sample solution was diluted twice for UPLC-QTOF/MS.

V. coloratum powder (30 g) was immersed in a 1000 mL flask with 500 mL of distilled water and extracted for 6 h in an essential oil extractor. n-hexane was used as solvent in the essential oil extractor. The solution in the flask was kept slightly boiling during the extraction process. After cooling to ambient temperature, the extract was collected to a 5 mL volumetric flask, and the essential oil extractor was washed twice with n-hexane, which was then added to the extract. n-hexane was added to the volumetric flask until the total volume reached 5 mL. The extract was analyzed by GC after filtering through a 0.22 μm membrane.

2.4. HPLC analysis

A Shimadzu HPLC system, with an LC20ATvp pump coupled with an SPD-20Avp UV-detector (Shimadzu Corp., Kyoto, Japan), was used to analyze the 50% methanol extracts. HPLC analysis was performed according to the previous study [27].

2.5. GC analysis

The assay was performed on an Agilent 6890 N gas chromatograph with a FID (Agilent Corp., Palo Alto, CA, USA). Separation of volatile components was carried out on a PEG-20 M capillary gas chromatographic column (30 m \times 0.32 mm \times 0.6 μm). The injection volume was 2 μL . The injections were conducted in split mode with a split ratio of 5:1 under the conditions: injector at 250 $^{\circ}\text{C}$, column oven at 60 $^{\circ}\text{C}$ for 3 min, programmed at a rate of 3 $^{\circ}\text{C}/\text{min}$ to 130 $^{\circ}\text{C}$ and then raised to 210 $^{\circ}\text{C}$ at a rate of 2.5 $^{\circ}\text{C}/\text{min}$. Nitrogen served as the carrier gas at 1.2 mL/min.

2.6. UPLC-QTOF/MS analysis

The ACQUITY UHPLC system equipped with the Xevo G2-XS QTOF (Waters Corp., Milford, MA, USA) in ESI-positive ionisation mode was used. The separation was carried out using an ACQUITY UPLC@BEH C₈ column (2.1 mm \times 100 mm, 1.7 μm), and the mobile phase included 0.1% formic acid (A) and acetonitrile (B). The elution gradient program was as follows: 0–9 min, 10%–40% B; 9–15 min, 40%–85% B; 15–20 min, 85%–85% B; 20–20.5 min, 85%–10% B; 20.5–22 min, 10%–10% B; flow rate was 0.25 mL/min. The injection volume was 10 μL . The column temperature was kept at 35 $^{\circ}\text{C}$.

For mass spectrometry detections, data were acquired using sensitivity mode with resolution >22,000 FWHM under positive electrospray ionisation. Acquisition range was 50–1000 *m/z*. Capillary voltage was 3 kV. Cone voltage was 30 V. The temperatures of source and desolvation gas were maintained at 150 $^{\circ}\text{C}$ and 450 $^{\circ}\text{C}$, respectively, cone gas flow at 50 L/h and desolvation gas flow at 800 L/h. An alternation of low-energy (collision cell energy of 6 V) and elevated energy (collision cell energy ramped from 10 to 30 V) acquisition was used to obtain the precursor ion (MS) and the fragmentation ion. The QC solution was obtained by mixing equal amounts of each sample solution and was injected once every 5 samples throughout the analytical run.

2.7. Data pre-processing and statistical analyses

The original HPLC-UV data and GC-FID data were respectively normalized, which produced a data matrix including the sample name (ID), retention time (t_R), and relative peak intensity.

The original multiple variables were transformed into a few comprehensive indicators (i.e., principal components (PCs)) by principal component analysis (PCA), thereby achieving feature extraction and visualization for large-scale complex data. Then, the processed data were imported in SIMCA 14.0 (Umetrics, Umea, Sweden) for further analysis through PCA with Pareto scaling mode, partial least squares discrimination analysis (PLS-DA), and orthogonal partial least squares discriminant analysis (OPLS-DA).

The UPLC-QTOF/MS raw data were processed on Progenesis QI 2.3 (Waters, Milford, MA, USA). The main procedures included chromatographic peak alignment, peak picking, normalisation, deconvolution, and compound identification. The 36 runs were aligned on the basis of an automatically selected QC. The selected adduct ions, including $[\text{M}-\text{H}_2\text{O}+\text{H}]^+$, $[\text{M}+\text{H}]^+$, $[\text{M}+2\text{H}]^+$, $[\text{M}+\text{NH}_4]^+$, $[\text{M}+\text{Na}]^+$, $[\text{M}+\text{K}]^+$ and $[\text{M}+\text{ACN}+\text{H}]^+$, were used to deconvolute the data. Subsequently, a matrix was generated, which contained aligned peaks with normalized peak intensities and sample numbers.

Data fusion was carried out on Matlab R2016a. The mid-level data fusion concatenates latent variables extracted from each data source into a single data set. This data set was then used for further multivariate classification. As the purpose of this study was to investigate the factors with greater influences (better classification), the unsupervised analysis (PCA) was adopted. At first, every raw data matrix was normalized using z-scores, and PCA was then applied for latent variable extraction. The scores of PCs from each data source were concatenated to obtain the fusion data, based on which PCA was performed subsequently [28].

2.8. Identification of characteristic components

Characteristic components were selected by five criteria: variable influence in projection (VIP) >1, $|\text{p}|>0.1$, $|\text{p}(\text{corr})|>0.5$ (correlation coefficient), ANOVA $P\leq 0.05$, and max fold change ≥ 2 . The first three parameters were calculated by OPLS-DA model, and the last two parameters were obtained from Progenesis QI.

On the basis of the abovementioned five criteria, the characteristic components were identified using a self-established *V. coloratum* compounds information database, which was established through references and querying databases such as SciFinder and PubMed. This database contains information regarding compound structure, precise molecular weight, and compound mass spectrum fragment information.

2.9. Evaluation of the antioxidant activity

A total of 0.15 g *V. coloratum* powder was vortexed for 2 min with 4 mL of 0.1 mol/L phosphate buffer (pH 7.2). After kept at room temperature for 1 h, the mixture was sonicated for 1 min. The mixture was then centrifuged at 13,000 r/min for 5 min. The supernatant was used for superoxide radical scavenging assay.

Superoxide radical scavenging activity was determined according to pyrogallol autoxidation method as previously reported [29]. In short, 0.1 mL of the test solution and 0.4 mL of pyrogallol (2.5 mmol/L) were added into 4.5 mL of Tris-HCl buffer (0.05 mol/L, pH 8.2). Then, the mixture was incubated for 4 min at 25 °C followed by recording the absorbance at 299 nm. The free radical scavenging potential (FRSP) was calculated according to the previously reported method.

DPPH free radical scavenging assay was performed according to the method previously reported [30]. In brief, a series of the *V. coloratum* sample solutions (1 mL) were dispensed into a 96-well plate with 2 mL of DPPH methanolic solution (0.2 mM). The absorbance at 517 nm was recorded up to 45 min in the dark. The dose-effect curve was plotted with the clearance rate as the ordinate and the concentration of the sample solution as the abscissa. The concentration of the sample at a clearance rate of 50% (IC_{50} , $\mu\text{mol/L}$) value was calculated based on the dose-response curve.

3. Results and discussion

3.1. HPLC-UV analysis

Typical chromatogram obtained from HPLC is shown in Fig. 2. The original HPLC-UV data were normalized in Excel, which generated a 51×30 data matrix including the sample number (ID), t_R , and relative peak intensity.

The 30 samples could be divided into two groups (CBM and CISR) according to their origin and divided into three groups (PO, SA, and UL) according to their host plant. PCA was performed to analyze the differences in metabolic profile of *V. coloratum*. The score plot is shown in Fig. 3.

The result of PCA showed that the samples from CBM and CISR groups were scattered into different regions while those from PO, SA and UL groups were located together, indicating that the metabolic profile of *V. coloratum* is affected by more the environment than the host.

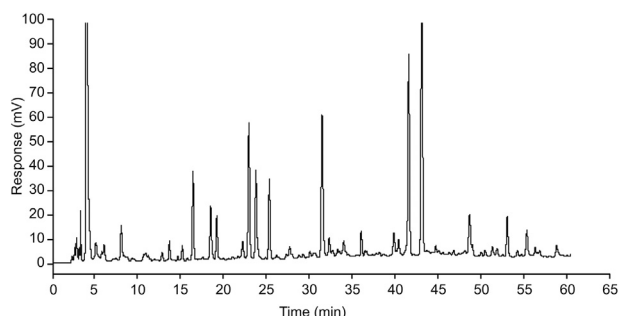


Fig. 2. Typical HPLC-UV fingerprint of *Viscum coloratum*.

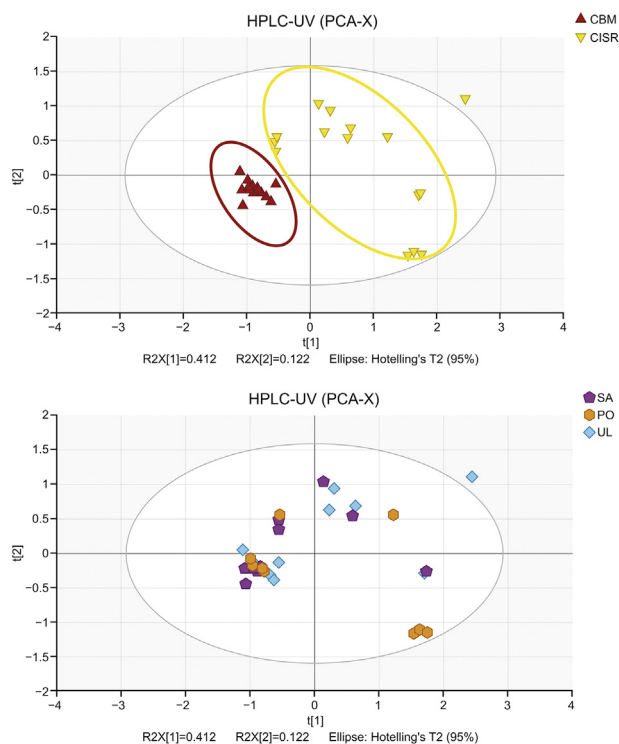


Fig. 3. Score plot of principal component analysis (PCA) for metabolic profile of *Viscum coloratum* obtained from HPLC-UV.

Samples in the CISR group were relatively scattered. This may be possibly attributed to the fierce competition for survival. The forests in Chengde Imperial Summer Resort are denser, and the fierce competition for survival and complex conditions of light and water resources may lead to a large difference in the growth of *V. coloratum*.

3.2. GC analysis

The typical chromatogram of GC is shown in Fig. 4. The original GC data were normalized in Excel, which generated a 51×30 data matrix including the sample name (ID), t_R and relative peak intensity. PCA was performed to analyze the data in the matrix. The score plot of PCA for GC metabolic profile is shown in Fig. 5.

As shown in Fig. 5, neither environment nor the host could clearly distinguish *V. coloratum* samples, but a separation trend was observed in both score plots. Therefore, the OPLS-DA model of each pair of comparative host groups and corresponding origin groups

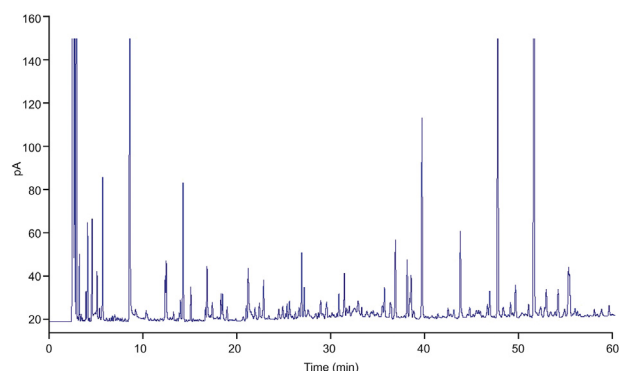


Fig. 4. Typical GC fingerprint of *Viscum coloratum*.

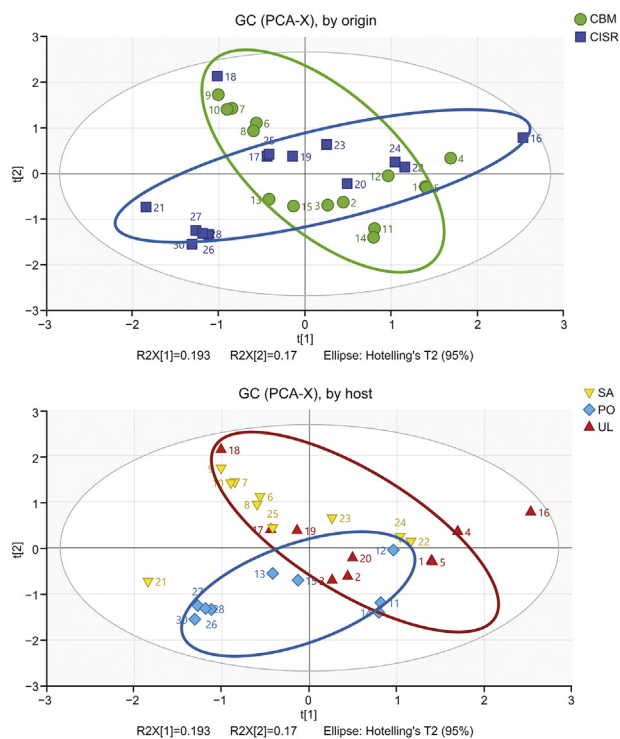


Fig. 5. Score plot of PCA for metabolic profile of *Viscum coloratum* obtained by GC.

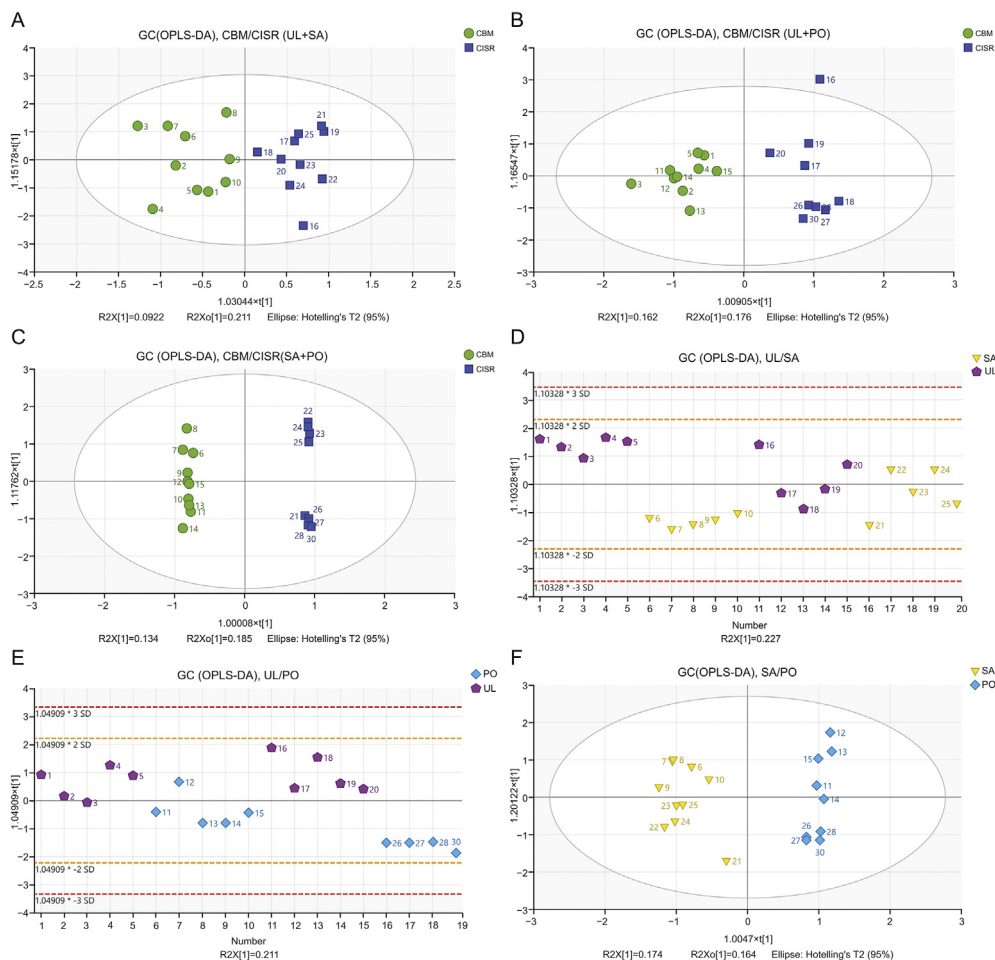


Fig. 6. Score plots of OPLS-DA for six comparative groups. (A) Changbai Mountain, Jilin province, China (CBM)/Chengde Mountain Resort, Hebei province, China (CISR) comparative group in UL and SA groups. (B) CBM/CISR comparative group in PO and UL groups. (C) CBM/CISR comparative group in PO and SA groups. (D) UL/SA comparative group. (E) UL/PO comparative group. (F) SA/PO comparative group.

was constructed. The score plots of six comparative groups (UL/SA, SA/PO, UL/PO and CBM/CISR in UL/SA, SA/PO and UL/PO) from OPLS-DA are shown in Fig. 6.

The effects of environment and host plants on metabolic profile were evaluated based on the quality of models, which was represented by R2X or R2Y and Q2 terms (Table 2).

In Table 2, Q2 represents the predictability of the model. R2X or R2Y represents the explanation proportion of variance. For all parameters, the closer to 1, the better the model.

An obvious separation between the CBM and CISR groups was observed in the score plots as shown in Figs. 6A–C, but no distinct separation could be seen between the UL and SA groups (Fig. 6D) or between the UL and PO groups (Fig. 6E). Although the samples from SA and PO groups were separated according to principal component 1 (t[1]) (Fig. 6F), they were separated better based on the sample origin (Fig. 6C).

The parameters (Table 2) of every CBM/CISR model were greater than those of the model constructed between host groups. Overall, the comparison results indicate that both environment and host influence the metabolic profile of *V. coloratum*, while different environments largely contribute to the changes of metabolic profile.

The volatile components, most of which are unstable and evaporable, were examined by GC-FID. Due to the fact that the current result can be affected by sample acquisition and storage time, the effect of the host plants and environment on the volatile components of *V. coloratum* requires further study.

Table 2
Parameters of six models.

No.	Type	N	R2X (cum)	R2Y (cum)	Q2 (cum)	Model
1	OPLS-DA	20	0.227	0.477	0.129	UL/SA
2	OPLS-DA	20	0.304	0.816	0.375	CBM/CISR in (UL + SA)
3	OPLS-DA	19	0.457	0.952	0.829	SA/PO
4	OPLS-DA	19	0.859	0.998	0.856	CBM/CISR in (SA + PO)
5	OPLS-DA	19	0.211	0.627	0.358	UL/PO
6	OPLS-DA	19	0.337	0.905	0.72	CBM/CISR in (UL/PO)

OPLS-DA: orthogonal partial least squares discriminant analysis.

3.3. UPLC-QTOF/MS analysis

3.3.1. Multivariate statistical analysis

A typical UPLC-QTOF/MS chromatogram is shown in Fig. 7. The raw data were imported in Progenesis Q1 2.3 (Waters, Milford, MA,

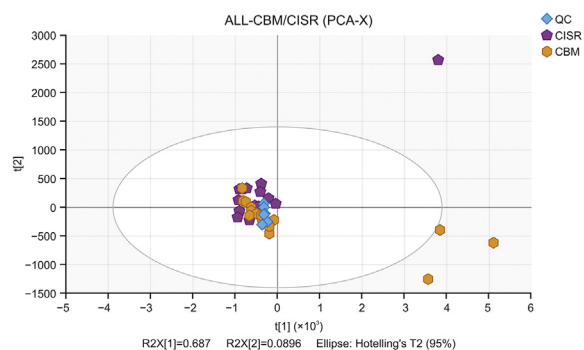


Fig. 8. Score plot of PCA for metabolic profile of *Viscum coloratum* obtained from UPLC-QTOF/MS.

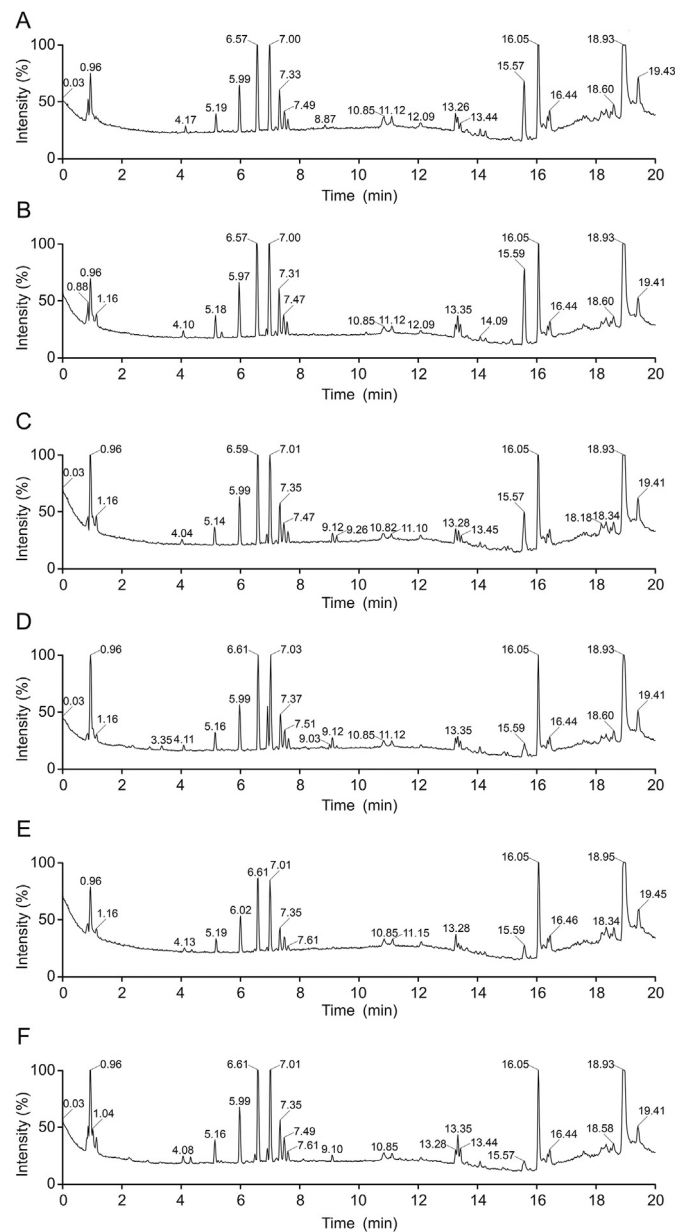


Fig. 7. Typical positive TIC chromatograms of *Viscum coloratum*. (A) Host on PO from CISR, (B) host on UL from CISR, (C) host on SA from CISR, (D) host on UL from CBM, (E) host on PO from CBM, and (F) host on SA from CBM.

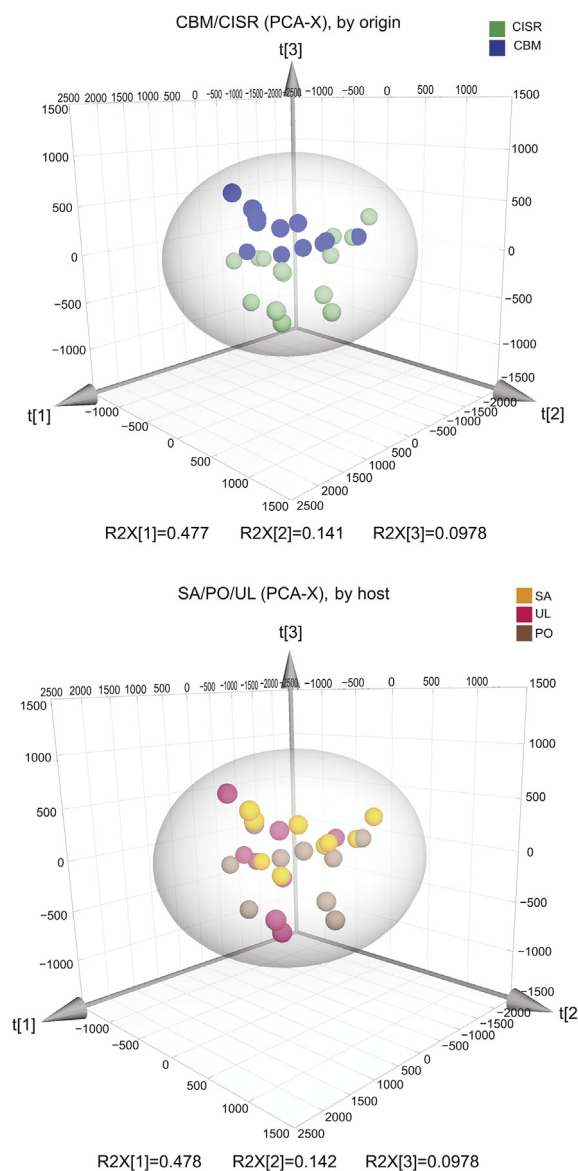


Fig. 9. 3D score plot of PCA for metabolic profile of *Viscum coloratum* analyzed by UPLC-QTOF/MS.

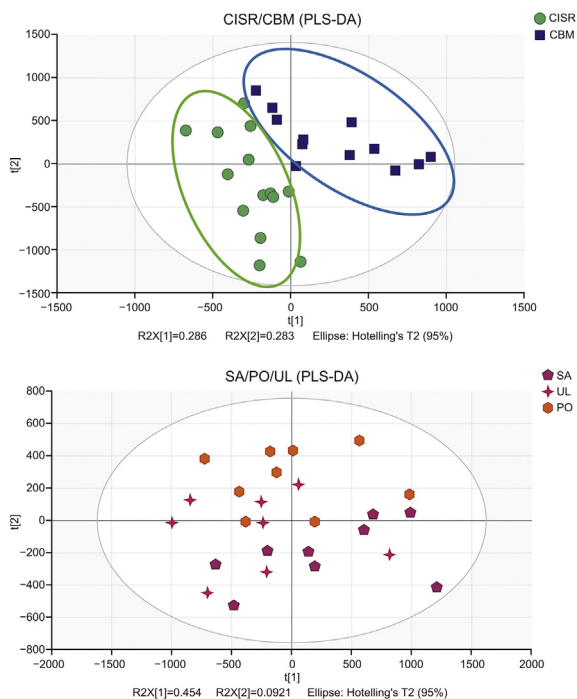


Fig. 10. Score plot of partial least squares discrimination analysis (PLS-DA) for metabolic profile of *Viscum coloratum* obtained from UPLC-QTOF/MS.

USA) for data processing, in which a $10,383 \times 36$ data block including the sample number (ID), t_R , and relative peak intensity was generated.

PCA was used to analyze the data. The score plot from PCA (Fig. 8) shows that the QC samples were clustered closely together located at the centre, indicating that the system stability was excellent. Moreover, four samples (Nos. 1, 5, 15, and 24) were outside the range of the ellipse, indicating that these samples were outliers. Therefore, the remaining samples excluding Nos. 1, 5, 15 and 24 were used in further analyses.

The score plot of PCA excluding outliers (Fig. 9) showed a good separation pattern between the CISR and CBM groups, while no obvious separation was observed among the UL, SA and PO groups, indicating that the metabolites are more affected by the environment than by the host.

PLS-DA was used to differentiate the metabolic profiles between the CBM and CISR groups and among the PO, SA and UL groups. As shown in Fig. 10, samples were divided into two groups according to habitats, while the samples were clustered when grouped by hosts. All parameters of these models are summarised in Table 3. Obviously, the model parameters of CBM/CISR had significantly higher values, whereas the model of SA/PO/UL had lower values of goodness of fit, with Q^2 (cum) < 0 and $R^2Y = 0.336$. This result indicated that the metabolites in *V. coloratum* were more affected

Table 3
Parameters of five models.

No.	Type	N	R2X (cum)	R2Y (cum)	Q2 (cum)	Title
1	PCA-X	36	0.777		0.619	ALL
2	PCA-X	26	0.618		0.574	/
3	PLS-DA	26	0.569	0.709	0.603	CBM/CISR
4	PLS-DA	26	0.547	0.336	-0.00074	SA/PO/UL
5	OPLS-DA	26	0.569	0.709	0.572	CBM/CISR

PCA: principal component analysis; PLS-DA: partial least squares discrimination analysis.

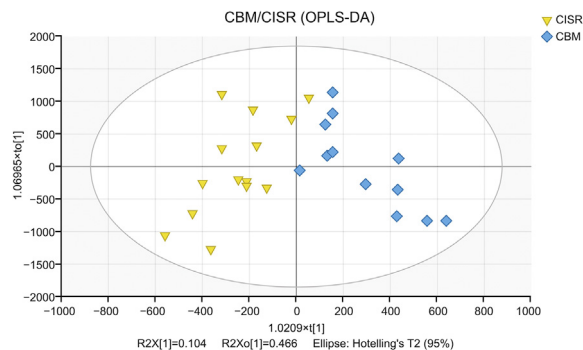


Fig. 11. Score plot of OPLS-DA for metabolic profile of *Viscum coloratum* obtained from UPLC-QTOF/MS.

by the environment than the host plant. Therefore, differential metabolites were screened between CBM and CISR.

3.3.2. Identification of characteristic components

Different metabolites between CBM and CISR groups were analyzed using OPLS-DA. Score plots are presented in Fig. 11.

Characteristic components were screened based on the criteria described in Section 2.8. Ten differential metabolites were screened according to the five standards, and three compounds were identified using a self-established *V. coloratum* compounds information database (Table 4 and Fig. 12).

3.3.3. Data fusion

The latent variables (PCs) were obtained by PCA analysis on three data blocks from HPLC-UV, GC-FID, and UPLC-QTOF/MS. As a result, PC1 and PC2 in HPLC-UV, GC-FID, and UPLC-QTOF/MS explained 56.19%, 52.24%, and 69.64% variances, respectively.

Mid-level data fusion was carried out according to the combination of PCs scores from each data block. Subsequently, PCA was performed on the fused data. The model generated similar results compared with those of the separate analysis. Most samples were clearly classified according to origin (Fig. 13), while they were fused together in accordance with their hosts (Fig. 14). The results of the comprehensive analysis of the data from three platforms indicated that origin accounts for the main influential source, which is consistent with the results from the separate analysis.

3.4. Antioxidant activity

The results from the antioxidant assay of the 30 samples are listed in Table 5. The effects of environment and host plants on the antioxidant activity of *V. coloratum* were determined by two-way ANOVA using IBM SPSS Statistics (IBM, Armonk, NY, USA). The results (Table 6) suggest that the environment exerts a significant impact on the antioxidant activity ($P < 0.05$). This finding is consistent with the results from metabolic analysis, which indicated that the quality of *V. coloratum* in the CBM group might be better.

Türe et al. [31] studied the nutritional relationships between mistletoes and its hosts in different habitats, and found that the nutrient absorption of mistletoes from the hosts is mainly influenced by the type of habitat. Scalon et al. [32] found that temperature and humidity significantly affect nitrogen concentration and carbon isotopic composition of leaves in mistletoes and host plants. Moreover, they also suggested that nutrient absorption by mistletoes is closely related to the type of habitat.

Aside from the nutritional characteristics, the numbers of *V. coloratum* on hosts reveal important information for evaluating

Table 4
UHPLC-QTOF/MS data of the characteristic components in *Viscum coloratum* between CBM and CISR groups.

No.	Compounds	Retention time (min)	[M+H] ⁺ and fragments (m/z)			Elemental composition	
			Calculated	Observed	Error (ppm)		
1	Homoeriodictyol-7-O-β-D-aposiyl-(1 → 2)-O-β-D- glucoside	6.89	597.1819	597.1830	1.84	C ₂₇ H ₃₃ O ₁₅	
			303.0869	303.0844	-8.25		C ₁₆ H ₁₅ O ₆
2	Homoeriodictyol	6.89	303.0869	303.0856	-4.29	C ₁₆ H ₁₅ O ₆	
			153.0188	153.0171	-11.11		C ₇ H ₅ O ₄
3	Homoeriodictyol-7-O-β-D-glucoside	6.89	465.1397	465.1379	-3.87	C ₂₂ H ₂₅ O ₁₁	
			303.0869	303.0854	-4.95		C ₁₆ H ₁₅ O ₆

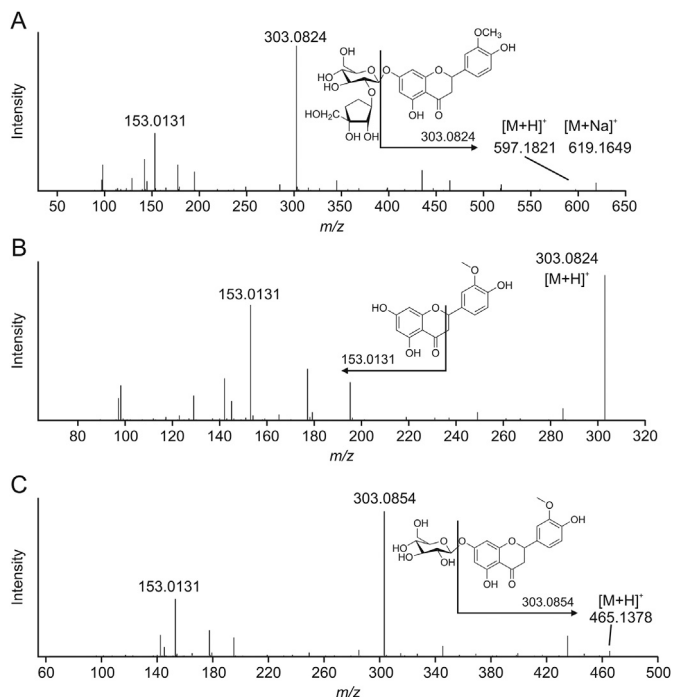


Fig. 12. Fragmentation trace for (A) compounds 6.89_596.1757n, (B) 6.89_302.0625n, and (C) 6.89_464.1294n.

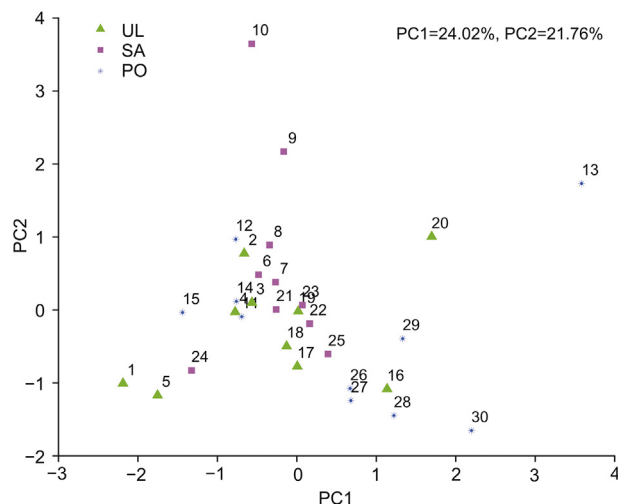


Fig. 14. Scores plot from PCA group by host for mid-level data fusion.

Table 5
Antioxidant activity of *Viscum coloratum* grown on different hosts and origins.

No.	O ₂ ^{-•} FRSP (%)	DPPH IC ₅₀ (μg/mL)	No.	O ₂ ^{-•} FRSP (%)	DPPH IC ₅₀ (μg/mL)
1	54.26	4.746	16	28.81	11.893
2	34.34	4.480	17	35.22	11.728
3	29.70	0.996	18	32.07	1.106
4	51.96	11.321	19	36.80	4.325
5	50.79	3.200	20	34.19	7.286
6	31.38	1.166	21	34.29	6.789
7	33.25	1.193	22	34.00	22.962
8	36.31	1.194	23	33.45	8.609
9	37.35	1.686	24	35.13	13.225
10	38.28	2.952	25	52.94	16.905
11	45.62	6.837	26	35.22	11.321
12	38.97	4.301	27	32.91	10.506
13	50.00	8.580	28	37.84	13.115
14	45.17	1.105	29	33.50	6.144
15	44.89	1.002	30	32.61	8.657

FRSP: free radical scavenging potential.

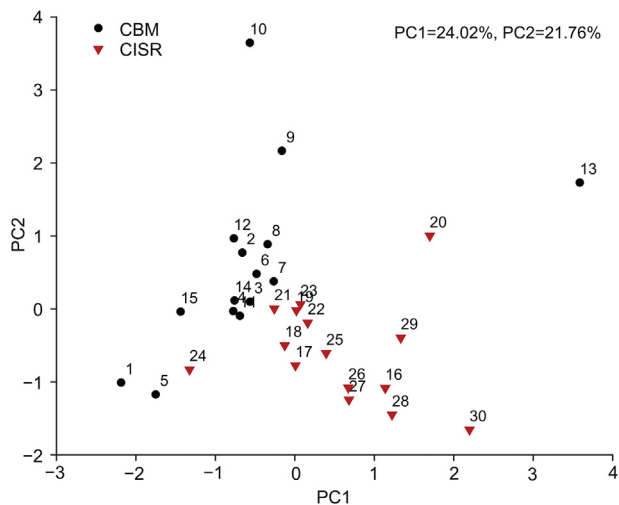


Fig. 13. Scores plot from PCA group by origin for mid-level data fusion.

environmental factors. Improvements in *V. coloratum* greatly depends on the ability to absorb water and minerals from their host plants [33]. Hosts may make an attempt to make up for the increased nutritional requirements of *V. coloratum* by acquiring more nutrients from the environment [34]. Generally, nutrients are easily absorbed by host plants in areas with abundant water resources; therefore, the nutrition potential of *V. coloratum* from the hosts is mainly affected by the type of habitat. CBM is covered with original dense forests and rich water resources, whereas CISR is with a semi-arid habitat. Considering the findings from this study, we believe that host plants

Table 6
Two-way analysis of variance of antioxidant activity.

Source	Dependent variable	Sum of squares	df	Mean square	F	P
Habitats	O ₂ ^{•-}	290	1	290	7.35	0.012
	DPPH	332	1	332	20.2	0.000
Host species	O ₂ ^{•-}	48.9	2	24.5	0.620	0.546
	DPPH	12.6	2	6.33	0.385	0.684
Habitats × Host species	O ₂ ^{•-}	295	2	147	3.74	0.039
	DPPH	123	2	61.5	3.74	0.038
Error	O ₂ ^{•-}	947	24	39.4		
	DPPH	394	24	16.4		
Total	O ₂ ^{•-}	4.58 × 10 ³	30			
	DPPH	2.32 × 10 ³	30			

and environment can have influence on the secondary metabolism and antioxidant activity of *V. coloratum*, while the influence of environment is greater than that of host plants.

4. Conclusions

The metabolite profile of *V. coloratum* is simultaneously affected by host plant and environment, and the environment factors play a key role in the synthesis and accumulation of the metabolites. Meanwhile, three main differential metabolites between two environment groups are identified. The results of antioxidant activity assay indicated that the biological activity of *V. coloratum* is more affected by the environment factors as well, and the quality of *V. coloratum* in CBM may be better.

Overall, various chemical analysis methods can provide multi-dimensional metabolite profile information for the integral quality evaluation. This study may provide new ideas and references for the quality control of semi-parasitic herbal medicine.

CRedit author statement

Rui-Zhen Zhang: Conceptualization, Methodology, Software, Formal analysis, Writing - Original draft preparation; **Jing-Tao Zhao:** Investigation, Formal analysis; **Wei-Qing Wang:** Investigation, Methodology; **Rong-Hua Fan:** Formal analysis; **Rong Rong:** Methodology; **Zhi-Guo Yu:** Resources, Supervision; **Yun-Li Zhao:** Writing - Reviewing and Editing, Supervision, Funding acquisition, Project administration.

Declaration of competing interest

The authors declare that there are no conflicts of interest.

Acknowledgments

This research was funded by the National Natural Science Foundation of China (Grant No.: 30901967), the Natural Science Foundation of Liaoning Province (Grant No.: 2013020223), and Shenyang Pharmaceutical University Student Science and Technology Innovation Project (Grant No.: 12). We would like to thank TopEdit (www.topeditsci.com) for English language editing as well.

References

- [1] M.E. Rodríguez-Cruz, L. Pérez-Ordaz, B.E. Serrato-Barajas, et al., Endothelium-dependent effects of the ethanolic extract of the mistletoe *Psittacanthus calyculatus* on the vasomotor responses of rat aortic rings, *J. Ethnopharmacol.* 86 (2003) 213–218.
- [2] M. Radenkovic, V. Ivetic, M. Popovic, et al., Effects of mistletoe (*Viscum Album L.*, Loranthaceae) extracts on arterial blood pressure in rats treated with atropine sulfate and hexocycline, *Clin. Exp. Hypertens.* 31 (2009) 11–19.
- [3] E. Suveren, G.F. Baxter, A.B. Iskit, et al., Cardioprotective effects of *Viscum album L.* subsp. *album* (European mistletoe) leaf extracts in myocardial ischemia and reperfusion, *J. Ethnopharmacol.* 209 (2017) 203–209.
- [4] D.D. Orhan, M. Aslan, N. Sendogdu, et al., Evaluation of the hypoglycemic effect and antioxidant activity of three *Viscum album* subspecies (European mistletoe) in streptozotocin-diabetic rats, *J. Ethnopharmacol.* 98 (2005) 95–102.
- [5] M. Majeed, K.R. Hakeem, R.U. Rehman, Mistletoe lectins: from interconnecting proteins to potential tumour inhibiting agents, *Phytomedicine Plus* 1 (2021), 100039.
- [6] M. Giudici, J.A. Poveda, M.L. Molina, et al., Antifungal effects and mechanism of action of viscotoxin A3, *FEBS J.* 273 (2006) 72–83.
- [7] A. Coulon, E. Berkane, A.M. Sautereau, et al., Modes of membrane interaction of a natural cysteine-rich peptide: viscotoxin A3, *Biochim. Biophys. Acta* 1559 (2002) 145–159.
- [8] M.B. Enesel, I. Acalovschi, V. Grosu, et al., Perioperative application of the *Viscum album* extract Isorel in digestive tract cancer patients, *Anticancer Res.* 25 (2005) 4583–4590.
- [9] M.A. Alam, P.K. Naik, Impact of soil nutrients and environmental factors on Podophyllotoxin content among 28 *Podophyllum Hexandrum* populations of northwestern Himalayan region using linear and nonlinear approaches, *Commun. Soil Sci. Plant Anal.* 40 (2009) 2485–2504.
- [10] L.C. Olsson, M. Veit, G. Weissenböck, et al., Differential flavonoid response to enhanced UV-B radiation in brassica napus, *Phytochemistry* 49 (1998) 1021–1028.
- [11] G.M. Jochum, K.W. Mudge, R.B. Thomas, Elevated temperatures increase leaf senescence and root secondary metabolite concentrations in the understorey herb *Panax quinquefolius* (Araliaceae), *Am. J. Bot.* 94 (2007) 819–826.
- [12] Q. Li, S. Lei, K. Du, et al., RNA-seq based transcriptomic analysis uncovers α -linolenic acid and jasmonic acid biosynthesis pathways respond to cold acclimation in *Camellia japonica*, *Sci. Rep.* 6 (2016), 36463.
- [13] Y. Li, D. Kong, Y. Fu, et al., The effect of developmental and environmental factors on secondary metabolites in medicinal plants, *Plant Physiol. Biochem.* 148 (2020) 80–89.
- [14] J.I. Yoder, Parasitic plant responses to host plant signals: a model for subterranean plant–plant interactions, *Curr. Opin. Plant Biol.* 2 (1999) 65–70.
- [15] M. Bowie, D. Ward, Water and nutrient status of the mistletoe *Plucosepalus acaciae* parasitic on isolated Negev Desert populations of *Acacia raddiana* differing in level of mortality, *J. Arid Environ.* 56 (2004) 487–508.
- [16] D.Y. Okubamichael, M.E. Griffiths, D. Ward, Host specificity, nutrient and water dynamics of the mistletoe *Viscum rotundifolium* and its potential host species in the Kalahari of South Africa, *J. Arid Environ.* 75 (2011) 898–902.
- [17] R. Liu, B. Su, F. Huang, et al., Identification and analysis of cardiac glycosides in Loranthaceae parasites *Taxillus chinensis* (DC.) Danser and *Scurrula parasitica* Linn. and their host *Nerium indicum* Mill., *J. Pharm. Biomed. Anal.* 174 (2019) 450–459.
- [18] R. Piwowarczyk, I. Ochmian, S. Lachowicz, et al., Phytochemical parasite-host relations and interactions: a *Cistanche armena* case study, *Sci. Total Environ.* 716 (2020), 137071.
- [19] S.I. Vicaș, D. Rugină, L. Leopold, et al., HPLC fingerprint of bioactive compounds and antioxidant activities of *Viscum album* from different host trees, *Not. Bot. Hort. Agrobot. Cluj* 39 (2011) 48–57.
- [20] Y. Zhao, Z. Yu, R. Fan, et al., Simultaneous determination of ten flavonoids from *Viscum coloratum* grown on different host species and different sources by LC-MS, *Chem. Pharm. Bull. (Tokyo)* 59 (2011) 1322–1328.
- [21] C. Long, R. Fan, Q. Zhang, et al., Simultaneous identification and quantification of the common compounds of *Viscum coloratum* and its corresponding host plants by ultra-high performance liquid chromatography with quadrupole time-of-flight tandem mass spectrometry and triple quadrupole mass spectrometry, *J. Chromatogr. B Anal. Technol. Biomed. Life Sci.* 1061–1062 (2017) 176–184.
- [22] C.-D. Qian, Y.-H. Fu, F.-S. Jiang, et al., *Lasiodiplodia* sp. ME4-2, an endophytic fungus from the floral parts of *Viscum coloratum*, produces indole-3-carboxylic acid and other aromatic metabolites, *BMC Microbiol.* 14 (2014), 297.
- [23] S. Hayashi, E. Miyamoto, K. Kudo, et al., Comparison of the volatile components of three mistletoes, *J. Essent. Oil Res.* 8 (1996) 619–626.
- [24] Y. Li, Y.-L. Zhao, Y.-P. Yang, et al., Chemical constituents of *Viscum album* var. *meridianum*, *Biochem. Systemat. Ecol.* 39 (2011) 849–852.
- [25] R. Fan, Y. Ma, H. Yuan, et al., A new flavonoid glycoside and four other chemical constituents from *Viscum coloratum* and their antioxidant activity, *Heterocycles* 89 (2014) 1455–1462.
- [26] E. Borrás, J. Ferré, R. Boqué, et al., Data fusion methodologies for food and beverage authentication and quality assessment - a review, *Anal. Chim. Acta* 891 (2015) 1–14.
- [27] Y.-L. Zhao, R.-H. Fan, H.-X. Yuan, et al., Development of the fingerprints for the quality evaluation of *Viscum coloratum* by high performance liquid chromatography, *J. Pharm. Anal.* 1 (2011) 113–118.
- [28] S. Dai, Z. Lin, B. Xu, et al., Metabolomics data fusion between near infrared spectroscopy and high-resolution mass spectrometry: a synergetic approach to boost performance or induce confusion, *Talanta* 189 (2018) 641–648.
- [29] F. Meng, R. Chen, M. Zhang, et al., Extraction and antioxidant activity of polysaccharides from *Acanthopanax sicciosum* leaves, *Food Sci.* 31 (2010) 168–174.
- [30] L. Sun, D. Wang, Z. Zhang, 2,2-Diphenyl-1-picrylhydrazyl radical scavenging activities of eleven species of natural plant extracts, *Food Sci.* 30 (2009) 45–47.
- [31] C. Türe, H. Bökük, Z. Aşan, Nutritional relationships between hemi-parasitic

- mistletoe and some of its deciduous hosts in different habitats, *Biologia* 65 (2010) 859–867.
- [32] M.C. Scalon, I.J. Wright, A global analysis of water and nitrogen relationships between mistletoes and their hosts: broad-scale tests of old and enduring hypotheses, *Funct. Ecol.* 29 (2015) 1114–1124.
- [33] R.L. Mathiasen, D.L. Nickrent, D.C. Shaw, et al., Mistletoes: pathology, systematics, ecology, and management, *Plant Dis.* 92 (2008) 988–1006.
- [34] O. Miura, A.M. Kuris, M.E. Torchin, et al., Parasites alter host phenotype and may create a new ecological niche for snail hosts, *Proc. Biol. Sci.* 273 (2006) 1323–1328.